Developing a Ti6Al4V specimen to induce residual stress deformations and cracks for use in metal additive manufacturing online monitoring

Karabo Moore[1*], *Danie* Louw[2], and *Dean* Kouprianoff[1]

[1]Department of Mechanical and Mechatronic Engineering, Central University of Technology, South Africa, Free State, karabomoore@gmail.com, dkouprianoff@cut.ac.za
[2] National Laser Centre, Council for Scientific and Industrial Research, Meiring Naudè road, Brummeria, 0184, South Africa, DLouw@csir.co.za

Abstract

In laser powder bed fusion factors such as residual stresses within the part, lead to deformations and cracks which impact the quality of the final product. Although residual stress and deformations have been thoroughly studied research and development of in-situ online monitoring requires a specimen that cracks in a predictable manner. This paper aims to show which sample geometry can be used to replicate cracks. The Ti6Al4V sample was designed based on known residual stress phenomena from literature of rapid heating and cooling cycles inducing compressive and tensile stresses during L-PBF. The sample was developed with the aid of computer aided design and simulation software using the inherent strain method. For the purpose of consistency, two identical samples were built simultaneously, and for the purpose of repeatability, two different builds were conducted. It was shown that the sample failed as predicted by the simulations due to the effective plastic strain and equivalent stress exceeding that of the mechanical properties. The sample developed can be used to test if cracks that form during the L-PBF build process can be predicted and detected.

* Corresponding author: karabomoore@gmail.com

1 Introduction

Laser powder bed fusion (L-PBF) uses a laser to melt/sinter and fuse powder material together to form a part [1]. This type of AM method is commonly used for both rapid prototyping and production of metal or plastic parts. The quality of the metal parts in a L-PBF process depends on many factors such as the laser and material parameters, all of which in turn affect the resulting residual stresses [2]. Residual stresses in a material or object are those stresses that exist in the object without any application of external loads. Residual stresses are caused by the localised thermal heating and melting of the material by the laser during a L-PBF process [3]. Mercelis and Kruth, [4] describes these residual stresses with two mechanisms, the first one being the Temperature Gradient Mechanism in which during heating, the laser exposed layer expands due to the high temperatures but is restricted by the cold underlying layer/substrate, resulting in steep temperature gradients causing partially elastic and partially plastic compressive stress-strain conditions in the top layer. At instances these compressive stresses may be so high that they exceed the yield strength of the material, resulting in plastic compression of the top layer [5]. When the plastically compressed top layer reaches equilibrium with the surrounding environment, residual stresses are set up in the material. The second mechanism is the Cool Down Mechanism in which, when the irradiating laser beam is removed, the top surface shrinks, however, this shrinkage is restricted by the underlying layers which in result causes residual stress. Leuders et al. [6] studied the fatigue resistance and crack growth performance in Ti6Al4V samples and found that in contrast to crack initiation, which is influenced primarily by the pores, the main influencing factor on crack growth is the residual stress.

With an increase in implementation of AM technology in industry, there has also been a growing need for quality control measures. Deformations and cracks within the material caused by the residual stresses pose a quality assurance challenge for industries. Modern methods of attempting to address these challenges are in instances being implemented, and further investigated, such as the use of thermal based online monitoring techniques [7], acoustic emitted signal monitoring techniques [8], and build-plate sensors used by Hehr et.al. [9] which were used to detect the deformation and delamination of the parts during the L-PBF build process by means of a fibre optic sensor which measured the strains in the build-plate as the deformation occurred.

Although various L-PBF online monitoring techniques are being thoroughly investigated, there is a need for a sample that would fail in an anticipated timely manner, failure can at times be random, making it difficult for efficient monitoring, leading to large data being generated. The sample developed can be used to test the probability of detection capabilities of online monitoring techniques to detect failure in-situ and assist in efficient monitoring of deformations and cracks during the build process.

2 Methodology

Sample design and simulation

The geometry (shape, width, and height) of the sample was hypothesised based on known residual stress rapid heating and cooling phenomena from literature inducing tensile and compressive stresses during the build of the sample. The overall design of the shape of the sample was based on a cantilever sample that is cut to measure the deflection and infer residual stresses. The attachment points were modified based on simulations so that the upward curling of the sample tends to break at the attachment points. The area above the attachment points in Fig. 1. was designed to prompt the build-up of residual stresses. The

CAD sample was designed using SolidWorks 2021 and simulated using the inherent strain method with Simufact Additive 2020. To increase the accuracy of the simulations the cantilever deflections were used to calibrate the inherent strains. Three cantilevers were built on the EOS M290 and cut in the as-built condition. The deflections were measured and used to calibrate the inherent strains. The voxel size used for the calibration as well as the simulations was set to 0.25 mm. To ensure that failure is expected, different heights (indicated by h in Fig. 1) from 4mm to 6mm at 0.25mm increments were simulated. Each iteration was simulated to determine possible failure height based on the resulting stresses and strains.

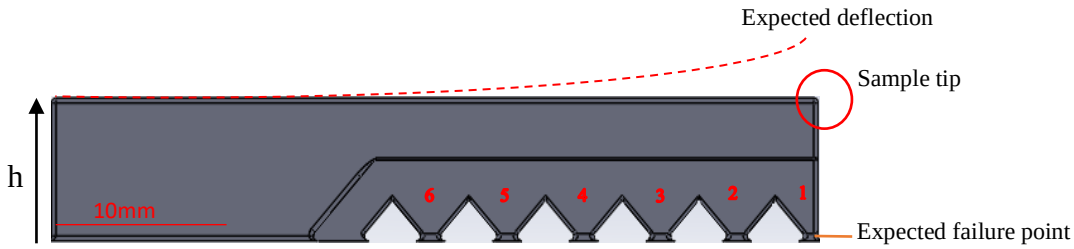

Fig. 1. CAD design of sample with indicated strut numbers

Manufacture of samples

The build of the sample was conducted using a EOSINT M290 L-PBF machine with standard process parameters for Ti6Al4V with a layer thickness of 40 µm. Extra Low Interstitial Ti6Al4V powder was used and a grade 5 Ti substrate. The machine parameters known from literature to have an effect on residual stresses, such as the laser power, scanning speed and scanning directions were kept constant. Two samples with identical geometries were build next to each other on the same build plate. The length and width being 45mm and 5mm respectively. The samples were visually monitored during processing. The layer at which failure occurred was identified by a sudden movement of the tip of the sample which resulted in the powder being flicked away from the tip. After failure was observed the building process was stopped. Thereafter, for the purpose of repeatability another build was performed with 2 identical samples.

3 Results and Discussion

Simulation results

In total eight different sample heights were simulated. The tensile material properties such as the yield stress, ultimate tensile strength and elongation of the sample is shown in Table 1 below. It can be seen from the table that an effective plastic strain around 8% and equivalent stress around 1280MPa would be required for the first strut to fail completely. The equivalent stress and effective plastic strain fields for the first strut of the initial three possible failure heights is shown in Fig. 2. It can be seen that the effective stress is close to the as-built ultimate tensile strength of ~ 1280 MPa when the sample height is at 5mm. Furthermore, the equivalent stress is above the yield stress of ~ 1120 MPa. when the sample height is at 4.5mm. It can also be seen from Fig.2. that the effective plastic strain reaches the strain at failure at a height of 4.75mm, which is ~ 8% for the material in this condition. Considering the observed mechanical properties of the sample, the simulation results indicate that a failure height of around 4.75mm can be expected of the first strut.

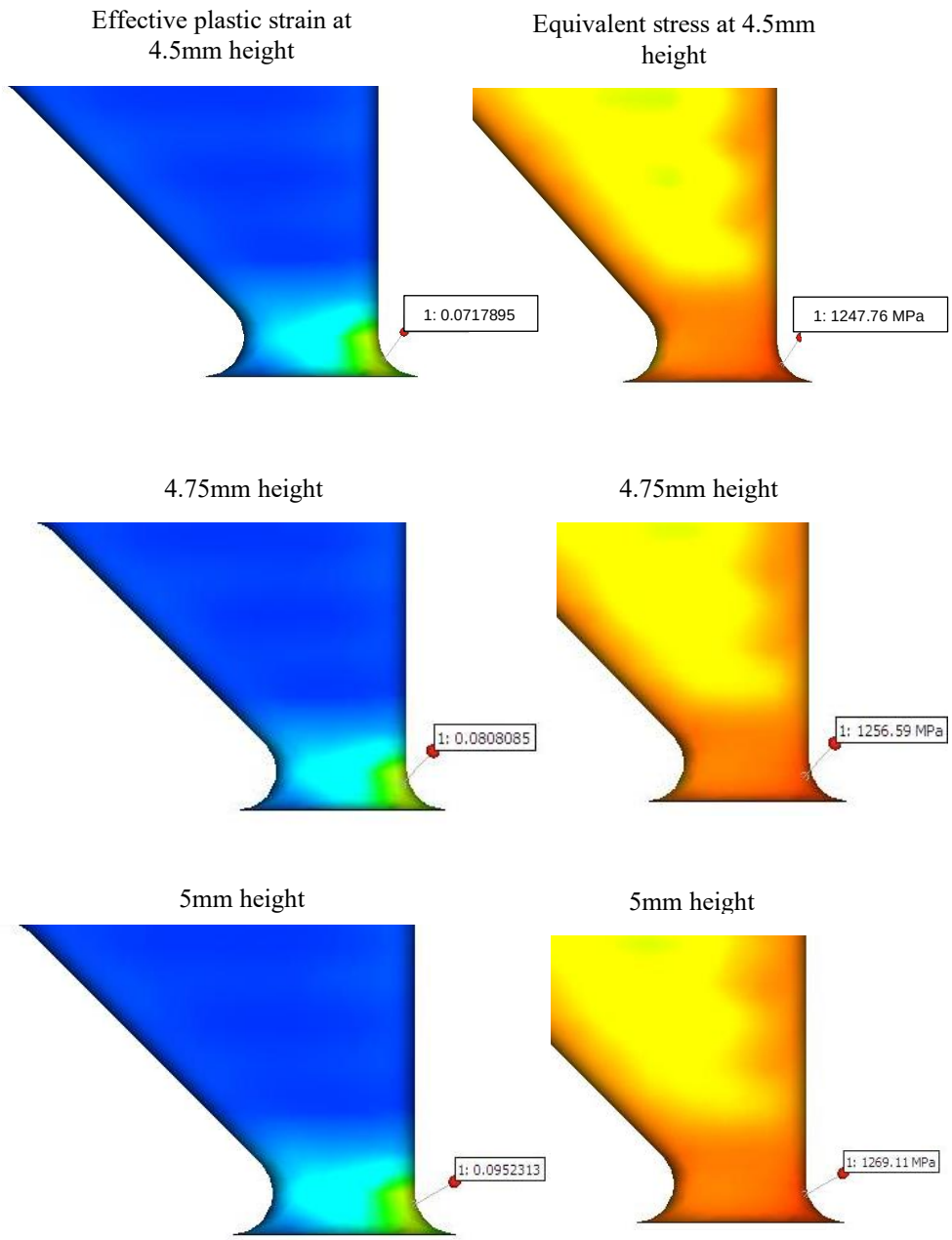

Fig. 2. Effective plastic strain (Left) and Equivalent stress (right) at three possible failure heights

Table 1: Ti6Al4V Tensile Results

	YIELD STRESS (MPa)	UTS (MPa)	ELONGATION (%)
AS BUILT	1198.49	1282.13	7.69

Strut failure

The two samples in the first build failed simultaneously at a height of 4.8mm. Interestingly in the second build one sample failed at a height of 4.7mm, while the second sample failed at 5.3mm. This deviation could be due to the dynamics of the gas flow in the chamber, slight cracking at the struts which causes local plastic deformation and in turn a reduction in stresses, or the thermal complexity of the L-PBF. The sudden movement of the sample as it cracked disturbed the surrounding powder as shown in Fig. 3. The sample height at which the denudation of the powder occurred was taken as the height at which failure occurred. It is seen from both the manufactured and simulated samples that predictions were accurate and a design height of ~ 6mm would be sufficient to ensure failure of the struts

.

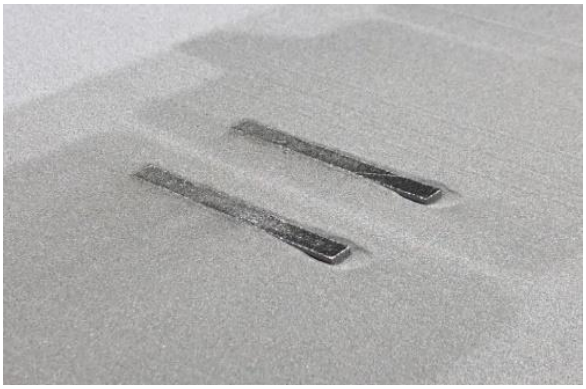

Fig. 3 Denudation in powder bed around tip of cantilever after failure

The upward deflection of samples due to the failure at the interface between the struts and the base plate from the propagated cracks is shown below in Fig. 4. In the enlarged section of the struts (Figure 4B), it can be seen that the last two struts (5 and 6) didn't fail, although strut 5 does have small cracks as seen in the Figure 4C.

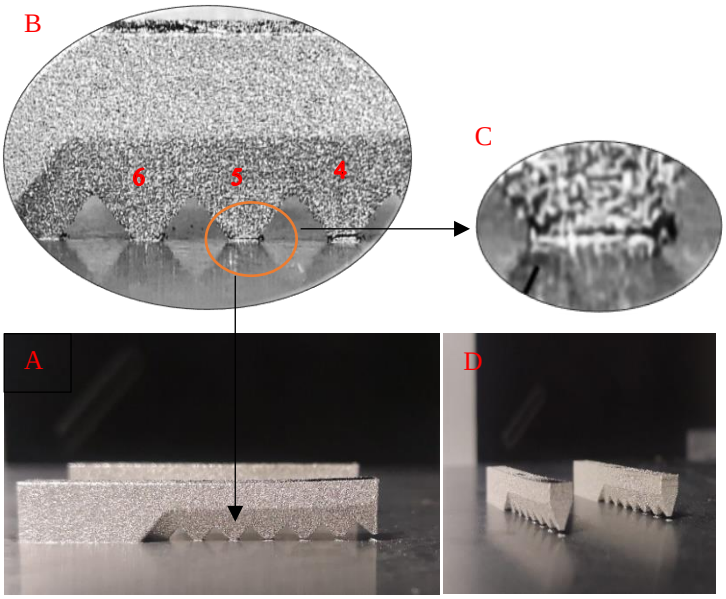

Fig. 4. Strut failure and deflection

Conclusion

This paper focused on developing a Ti6Al4V sample that would crack due to residual stress in an anticipated manner. During experiments, it was shown that the developed specimen can crack and deform as predicted by simulations using the inherent strain method. The samples of the first build failed simultaneously at a height close to the predicted failure height, although there were slight deviations observed in the failure of the second build of samples which would require further investigation. It was also observed through the simulations, that as the height of the sample was increased so did the effective stress and strain at the first strut. Online monitoring research is playing a fundamental role in the commercialization of the L-PBF technology in assuring quality products. The developed specimen can be used to reduce the time and cost of online monitoring research and development by producing predictable and repeatable deformations that can be monitored during the L-PBF process.

Acknowledgements

This research was supported by the Department of Science and Innovation (DSI) under the Collaborative Program in Additive Manufacturing (CPAM) contact number CSIR-NLC-CPAM-18-MOA-CUT-01. Thanks to the Centre for Rapid Prototyping and Manufacturing (CRPM) for their assistance.

References

[1] **S.K. Everton., M. Hirsch., P.I. Stravroulakis., R.K. Leach., A.T. Clare.,** 2016. Review of in-situ process monitoring and in-situ metrology for metal additive manufacturing. *Materials and Design* Elsevier Ltd, 95, pp. 431–445. doi:10.1016/j.matdes.2016.01.099.

[2] **I. Yadroitsev., P. Krakhmalev., I. Yadroitsava.,** 2015. Hierarchical design principles of selective laser melting for high quality metallic objects. Additive Manufacturing, 7, pp 45-56.

[3] **L. Mugwagwa., I. Yadroitsava., N.W. Makoana., I. Yadroitsev.,** (2021). Residual stress in laser powder bed fusion. In Fundamentals of Laser Powder Bed Fusion of Metals pp. 245–276. Elsevier. doi:10.1016/b978-0-12-824090-8.00014-7.

[4] **P. Mercelis., J. Kruth.,** 2006. Residual stresses in selective laser sintering and selective laser melting. Rapid Prototyping Journal, 12(5), pp. 254–265. Available at: http://www.scopus.com/inward/record.url?eid=2-s2.0-33750146493&partnerID=40&md5=7eebf030e96fa24df272aff5aea8f2cc.

[5] **K. Kempen., L. Thijs., B. Vrancken., S. Buls., J. Van Humbeek., J.P. Kruth.,** 2013. Lowering thermal gradients in selective laser melting by pre-heating the baseplate, in Solid Freeform Fabrication Symposium. Austin.

[6] **S. Leuders., M. Thöne., A. Riemer., T. Niendorf., T. Tröster., H.A. Richard., H.J. Maier**., 2013. On the mechanical behaviour of titanium alloy TiAl6V4 manufactured by selective laser melting: Fatigue resistance and crack growth performance. International Journal of Fatigue, 48, pp 300–307.

[7] **D. Tyralla., T. Seefeld.,** 2021. Thermal Based Process Monitoring for Laser Powder Bed Fusion, Advanced Materials Research, 1161, pp 123-130.

[8] **D. Kouprianoff., I. Yadroitsava., A. du Plessis., N. Luwes., I. Yadroitsev.,** (2021). Monitoring of Laser Powder Bed Fusion by Acoustic Emission: Investigation of Single Tracks and Layers. Frontiers in Mechanical Engineering, 7. pp 1-17 doi:10.3389/fmech.2021.678076.

[9] **A. Hehr., M. Norfolk., D. Kominsky., A. Boulanger., M. Davis., P. Boulware.,** 2020. Smart Build-Plate for Metal Additive Manufacturing Processes. Sensors, 20 (2), pp1-10. https://doi.org/10.3390/s20020360.